Convergence and Validation in ParaPower: A Design Tool for Phase Change Materials in Electronics Packaging

Michael Deckard, Patrick Shamberger
Texas A&M University,
College Station, Texas, United States of America, 77843
Email: patrick.shamberger@tamu.edu

Michael Fish, Morris Berman, Justin Wang, Lauren Boteler
U.S. Army Research Laboratory,
Adelphi, Maryland, United States of America, 20783
Email: lauren.m.boteler.civ@mail.mil

ABSTRACT

Integration of solid-liquid phase change materials (PCMs) into electronics packaging has demonstrated the potential to reduce the transient temperature rise of components that experience pulsed thermal loads. However, the impact on local temperature histories resulting from incorporating PCMs in different locations and configurations within an electronics package is not easy to analytically determine, due in large part to the non-linear response of PCMs to a transient heat load. ParaPower is a new parametric design tool to facilitate the design of electronics packages. The tool has the capability of easily incorporating arbitrarily located PCM volumes and evaluating their effect on temperature distributions within the electronics package as a function of time. This paper determines the spatial and temporal order of convergence for the reduced order phase-change thermal model which underlies ParaPower. The results are compared and validated against both an analytical solution and a higher-fidelity commercial finite element analysis (FEA) tool. This paper has shown the fast-solving methods used in the ParaPower tool give results with comparable accuracy to those obtained using high-fidelity commercial software. Reasonably good accuracy can be obtained with fairly large time steps and grid spacing allowing fast-solving design space exploration with this option to increase fidelity within the tool to obtain higher accuracy when necessary. This research quantifies the trade-off between time steps, grid size, and accuracy such that a useful balance can be obtained. Design tools, such as ParaPower, have the potential to significantly advance design theory to reduce size and cost as well as minimize the prevalence of overdesign.

KEY WORDS: phase change material, PCM, thermal management, simulation, modeling

NOMENCLATURE

A	area, m^2
E	error, °C
L_2	root mean square norm
L_∞	global maximum norm
N	number of gridpoints
Q	heat generation, W
R	resistance, Ω
T	temperature, K
c	constant pressure heat capacity
n	number of nodes
p	order of convergence, ratio
r	grid spacing or timestep ratio
v	volume
z	height

Greek symbols

Φ	melt fraction
ρ	density
Δt	timestep size

Subscripts

0	node being solved for
exact	exact analytical solution
i	neighboring node
j	any node
k	index of grid spacing or timestep dicretization
m	melting point

Superscripts

p	timestep

INTRODUCTION

Electronics have followed a continuous trend of miniaturization, steadily decreasing individual component size and increasing overall power density .[1] Thermal management of these increased power density remains an area of active research to prevent damage and increase efficiency in novel electronics packages.[2] In particular, periodic and/or transient heat generation present an additional level of difficulty in maximizing cooling loop efficiency. While a number of traditional and new thermal management techniques are capable of handling steady state heat generation, techniques to counter thermal transients remains difficult.[3,4] One technique that is popular in literature is to use phase change materials (PCMs) to absorb the thermal pulse. PCMs undergo a solid to liquid phase change and remain in a narrow temperature range during the course of the phase change. Coupled with a large latent heat of melting, PCMs have demonstrated potential as a thermal energy storage method, thereby mitigating temperature rise of a particular surface at a prescribed temperature for a period of time.[2,5,6]

Currently, few design tools exist capable of modeling the thermal impacts of implementing PCM materials. Commercial FEA packages are one such design tool, but these generally do not have the capability of rapidly modeling phase change and electrical properties simultaneously and, as commercial products, offer limited flexibility for incorporating new functionality within the tool. In order to facilitate optimum

electronics package design a parametric tool which is user-friendly and easily accessible is necessary. As an example of such, ParaPower is an open-access parametric design tool capable of modeling both steady-state and transient heat conduction and thermal stresses.[7,8], while simultaneous simulation of electrical properties will be added at a later date.ParaPower is not designed to replace high-fidelity commercial modeling tools but to act as an initial design tool to understand the parametric space. Assessing the parametric space can quickly become computationally expensive when sweeping various parameters: geometry, layout, materials, heat sink types, heat sink placement, etc. However, to achieve the most effective electronics package, it is important to understand how these various parameters interact with each other as well as their effect on temperature sensitivity. Many systems have overdesigned their thermal solutions to handle the peak load temperatures all the time even though they may only occur a small percentage of this time. By designing electronics packages and thermal solutions which account for both the average and peak heat loads, thermal overdesign can be reduced and system size and efficiency can be improved. The remainder of this paper will describe recent efforts to extend ParaPower to accurately simulate melting in distributed PCM volumes within an electronics package, and the validation of this portion of the parametric design tool.

ParaPower uses an implicit Euler finite difference scheme integrated with the 3D thermal resistance network to quickly calculate the temperatures in solid components in a user-defined rectilinear electronics module structure.[7-9] A single melting temperature enthalpy approach is used to determine the phase fraction of solid/liquid at an individual node within the PCM volume, where melting occurs at a single well-defined temperature.[10,11] This approach is implemented in MATLAB, and solves quickly, enabling fast, iterative thermal analyses and designs through parametric studies of the chip dimensions, number of chips, chip layout, material types, cooling solutions, etc. To ensure that the integration of the implicit finite difference scheme with a thermal resistance network can achieve a desired level of fidelity, convergence studies on two prototype models of increasing complexity are conducted: (1) transient heat-transfer/melting in a one dimensional system, and (2) spreading within a PCM-enhanced single-chip package. These results are compared against either the analytical solution for the Stefan problem (for the 1D case),[12,13] or the commercial finite element analysis (FEA) tool ANSYS Mechanical (for the 3D single-chip package) in which the apparent heat capacity method was used to spread the latent heat associated with melting over a finite-temperature mushy zone.[10]

ParaPower efficiently converges to the analytical solution of a two-region quasi-1D melting problem (L_2 norm < 0.1 °C, L_∞ norm < 0.2 °C) for grid sizes < 0.1 mm, and for time steps < 1 ms. Similar degrees of convergence are observed in more complicated 3D geometries by comparison with numerical results computed from commercial FEA code (ANSYS Mechanical), with computation time, t, scaling with grid spacing, N, as $t \sim N^2$. This indicates that the error associated with the nonlinearity of the melting model also tends towards zero with decreasing grid and time step. Having phase change incorporated and properly benchmarked provides an important extension to the functionality of ParaPower, allowing a comprehensive exploration of PCM-enhanced package design space with a rapid parametric modeling tool.

METHODS

Numerical Simulations

All simulations were performed within the ParaPower modeling software or ANSYS Mechanical. Army Research Labs (ARL) ParaPower is a Matlab-based simulation package developed at ARL utilizing the resistance model scheme,[7-9] in which simulation space is discretized into rectilinear volumetric elements. Each element is represented by a node in 3D space, with properties (specific heat, density, thermal conductivity) determined by the material and phase represented within the volume. These point values are connected rectilinearly to their nearest neighbors with a thermal resistance determined by the distance between nodes and the thermal resistivity of the point (Fig. 1), which satisfies the following relationship:

$$\sum_{i=1}^{6} \frac{1}{R_i}(T_i - T_0) = -Q_0, \qquad \text{Eq. 1}$$

where T_0 is the temperature of the node being solved for, and T_i are the temperatures of the six nearest neighbor nodes in the rectilinear grid, or the boundary wall temperature in the case of an exterior node. Q_0 is the heat generation (or sink) in the node, and R_i are the resistances between nodes calculated as a series resistance. ParaPower is capable of non-uniform discretization, and the program ensures that each volume element consists of only a single material composition. When defined as a phase change material (with appropriate solid and liquid material properties), these volume elements may melt or solidify.

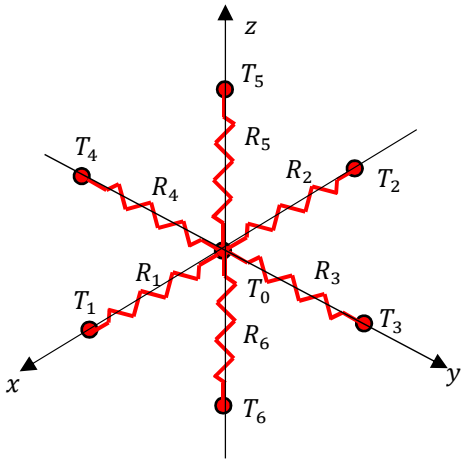

Fig. 1. Schematic of the nodal resistance network

ParaPower combines an implicit Euler scheme solver to determine the temperature at each timestep with an enthalpy-based method to account for melting / solidification occurring within a particular volume.[10,11] The implicit, or backward Euler method was selected due to its inherent stability. The equation for a single node is given by:

$$\sum_{i=1}^{6}\left(\frac{1}{R_i}\left(T_i^{p+1} - T_0^{p+1}\right)\right) - \frac{\rho_0^p c_0^p V_0}{\Delta t} T_0^{p+1} = -Q_0 - \frac{\rho_0^p c_0^p V_0}{\Delta t} T_0^p, \qquad \text{Eq. 2}$$

where the superscript p is the current timestep, $\rho, c,$ and V are the density, constant pressure heat capacity, and volume of the node, and Δt is the size of the timestep.

Node temperatures are modified at the end of each time step to account for endothermic melting (exothermic solidification). If the temperature of the PCM in a node $\left(T_{\mathrm{j}}^{\mathrm{p+1}}\right)$ exceeds the melting temperature of the PCM (T_{m}), and the PCM has not fully melted ($\phi < 1$), additional melting occurs, within the volume. The extent of additional melting is calculated by comparing the quantity of sensible heat above the melting point to the quantity of latent heat associated within the residual solid fraction following the standard enthalpy approach.[10,11] This process is reversed for the case of solidification.

Changes to the phase fraction are propagated to update the effective properties of the PCM nodes, based on difference in the solid and liquid material properties for the PCM. These changes are calculated after the melting/ solidification step, and affect the temperature calculation in the next timestep. After the updates to the material properties of the nodes is complete, the timestep is finished. The process is repeated for each timestep until the designated end timestep is reached.

Numerical approaches used in ParaPower are described in more detail in a previous work.[7-9]

Simulation Geometry

Three different geometries of PCM and underlying substrate structure were established to validate and test different aspects of the the ParaPower numerical tool.

A uniform slab of PCM heated from its base was defined within ParaPower, to determine convergence within ParaPower with grid spacing and time step, against an exact analytical solution for melting.[12,13] This geometry (*Geometry 1*) consisted of a 10 mm thick slab of Field's Alloy which was initially solid. Field's Alloy is an indium-bismuth-tin eutectic (51In-32.5Bi-16.5Sn, reported in wt%; $C_p = 250 \frac{\mathrm{J}}{\mathrm{kg \cdot K}}$, $k = 18.5 \frac{\mathrm{W}}{\mathrm{m \cdot K}}$) which was selected due to its appropriate melting temperature (T_m = 59 °C), and large thermal conductivity.[14,15] This alloy has been the subject of extensive testing as a PCM phase, including by co-authors of this manuscript.[5,6] A constant temperature boundary condition of 65 °C was applied to the bottom of the cube, and the remaining walls of the volume were adiabatic. The initial temperature of the volume was 55 °C. This resulted in propagation of a uniform melt front upwards through the volume that could be compared to the one dimensional analytical solution of a semi-infinite medium with a constant temperature boundary condition.[12,13] The number of nodes in the vertical direction ranged from 3^1 to 3^{10} (grid spacing of dz = 3.33 to 1.69×10^{-4} mm). The total simulated time was 1 s, with the total number of evenly spaced time steps ranging from 2^1 to 2^{13} (dt = 500 to 0.12 ms). Temperature was recorded as a function of height (z). Computational time is reported for a simulation performed on a computer with an Intel i7-7700 CPU at 3.60 GHz with 16 GB of RAM.

Two additional 3D geometries were simulated. Both of these geometries consist of a copper base plate with a silicon carbide (SiC) slab centered on top of the copper plate. The rest of the simulation space was composed of a low-melting point alloy (Field's Alloy). A planar heat generation of 200 W/cm^2 was generated on the top surface of the silicon carbide slab; the simulation walls were adiabatic. The entire volume is initially 0 °C. The total simulated time was 1 second. This allows enough time for portions of the low-melting point alloy to fully melt, while leaving other volumes partially melted or fully solidified. This facilitates testing all the phase change physics of the ParaPower program. *Geometry 2* had equal thickness Cu, SiC and alloy slabs to facilitate a comparison of convergence with different nodal spacings. The total volume is a cube of 30 mm per side, and the dimensions of the copper plate are 30 mm wide, 30 mm long, and 10 mm tall. The SiC slab is a cube of 10 mm per side (Fig. 2). The nodal grid density varied from 9×9×9 to 51×51×51 (grid spacing of dx = 3.33 to 0.59 mm), with number of evenly spaced time steps ranging from 2 to 33 (dt = 500 to 30.3 ms). These grid sizes allowed increasing refinement of the discretization while ensuring successive refinements had overlapping grid points necessary for convergence analysis.

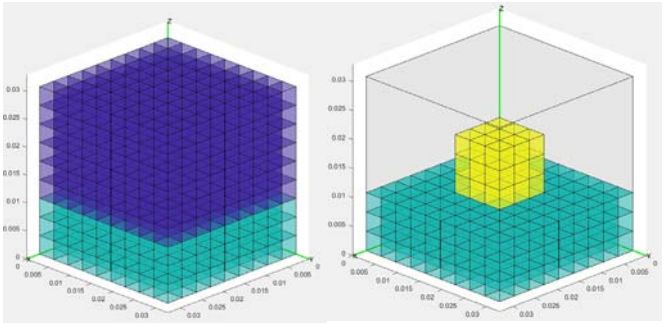

Fig. 2 Visualization of *Geometry 2* with the most course grid spacing detailing the Cu (blue), Field's Metal (purple – not shown in image to the right for clarity) and SiC (yellow) in the simulation.

Since ParaPower uses volume centered nodes, an odd numbered grid must be utilized to ensure that any grid points from successively courser grids lie on the same points as a finer grid. In addition, maintaining cubic volume elements forces equal refinements in all dimensions simultaneously, simplifying the analysis. The overall cubic shape of the simulation space and proportions of materials within *Geometry 2* were chosen so that overlapping grid points and cubic volume elements could be used across a wider range of grid sizes before simulations became impractical. The number of time steps per simulation ranged from 2 to 33 (dt = 500 to 30.3 ms) at which point further refinement became impractical. The time step size within a simulation remained constant for the duration of that simulation. These simulations were performed in parallel with 30 cores on Intel Xeon E5-2670 v2 CPUs with 64 GB of memory per node.

In *Geometry 3*, the heights of various components are adjusted to more closely resemble actual chip and base plate heights. The copper plate is 30 mm wide, 30 mm long, and 1 mm tall, the silicon carbide slab is 10 mm wide, 10 mm long, and 0.5 mm tall, and the simulation space is 30 mm wide, 30 mm long, and 2.5 mm tall. As above, the nodal grid density varied from 9×9×9 to 51×51×51 (grid spacing of dx = 3.33 to 0.59 mm), with 512 evenly space time steps (dt = 1.95 ms). This

simulation was performed in parallel with 40 cores on Intel Xeon E5-2698v4 CPUs with at least 128 GB of memory.

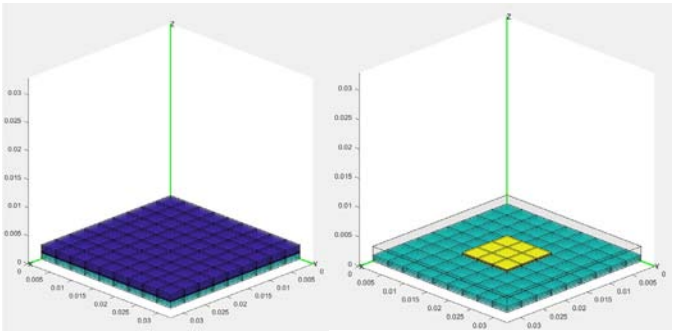

Fig. 3 Visualization of *Geometry 3* with the most course grid spacing shown, using the same color scheme as Fig. 2. Field's Alloy (which encapsulates the structure) is not shown in the image to the right for clarity.

Measures of Code Verification

Norms. Code verification, including convergence, was determined with use of the $\boldsymbol{L_2}$ and $\boldsymbol{L_\infty}$ norms. The $\boldsymbol{L_2}$ norm is the root mean square error across all N nodes between a particular temperature result and a reference case (either an analytical solution or a numerical model calculated at a finer grid or time resolution). The $\boldsymbol{L_2}$ norm is a commonly adopted global measure of fit between a particular solution, and a model output.[16] $\boldsymbol{L_2}$ is calculated as:[16]

$$L_{2,\mathrm{k}} = \sqrt{\frac{\sum_{\mathrm{j}=1}^{N} \left|T_{\mathrm{j,k}} - T_{\mathrm{j,exact}}\right|^2}{N}}, \qquad \text{Eq. 3}$$

when an analytical solution is used as a reference case, and

$$L_{2,\mathrm{k}} = \sqrt{\frac{\sum_{\mathrm{j}=1}^{N} \left|T_{\mathrm{j,k}} - T_{\mathrm{j,k+1}}\right|^2}{N}}, \qquad \text{Eq. 4}$$

for two numerical solutions. $\boldsymbol{T_{\mathrm{j,k}}}$, $\boldsymbol{T_{\mathrm{j,k+1}}}$ and $\boldsymbol{T_{\mathrm{j,exact}}}$ are the temperatures at node j, for a given grid spacing or time step, k, a more refined grid spacing or timestep $\boldsymbol{k+1}$ or the exact analytical solution.

The $\boldsymbol{L_\infty}$ norm is the maximum error occurring at any node within the volume between a particular temperature result and a reference case (either an analytical solution or a numerical model calculated at a finer grid or time resolution). The $\boldsymbol{L_\infty}$ norm is the worst pointwise discrepancy that occurs between two given models. Thus, the $\boldsymbol{L_\infty}$ norm is a measure of the maximum anticipated error that could occur at some particular critical location within a volume. $\boldsymbol{L_\infty}$ is calculated as:

$$L_{\infty,\mathrm{k}} = \max\left(\left|T_{\mathrm{j,k}} - T_{\mathrm{j,exact}}\right|\right) \qquad \text{Eq. 5}$$

for a numerical model and analytical solution or

$$L_{\infty,\mathrm{k}} = \max\left(\left|T_{\mathrm{j,k}} - T_{\mathrm{j,k+1}}\right|\right), \qquad \text{Eq. 6}$$

for two numerical solutions. In order to calculate either $\boldsymbol{L_2}$ or $\boldsymbol{L_\infty}$, the discretization must be made in such a way that a significant number of grid points for both models coincide, as only the common points between the two models can be used to calculate $\boldsymbol{L_2}$ or $\boldsymbol{L_\infty}$.

Order of Convergence. The order of convergence compares the $\boldsymbol{L_2}$ or $\boldsymbol{L_\infty}$ norms as a ratio to determine how quickly the error between models decreases as the discretization is refined. The order of convergence represents the rate at which the accuracy increases as the discretization is refined. These refinements can be with respect to grid spacing or time step. The order of convergence can calculated for either the $\boldsymbol{L_2}$ or $\boldsymbol{L_\infty}$ norm as follows:[16]

$$p_2 = \frac{\ln\left(\frac{L_{2,k+1}}{L_{2,k}}\right)}{\ln r}, \qquad \text{Eq. 7}$$

for comparison to the $\boldsymbol{L_2}$ norm, and

$$p_\infty = \frac{\ln\left(\frac{L_{\infty,k+1}}{L_{\infty,k}}\right)}{\ln}, \qquad \text{Eq. 8}$$

for comparison to the $\boldsymbol{L_2}$ norm, where p is the order of convergence, k denotes a given grid size or time step, $\boldsymbol{k+1}$ is a more finely discretized grid size or time step, and r is the ratio of either the grid sizes or time steps used. When the norms that are used calculate the order of convergence do not originate from comparison to an exact solution, it is called the observed order of convergence. The higher the order of convergence, the greater the decrease in error for a given discretization refinement. A positive order of convergence is a necessary criteria for validation of the model, and matching the theoretical order of convergence for the solver is strong evidence for model validation.[16] Negative orders of convergence may indicate problems with the underlying implementation of physics in the code.

RESULTS

Comparison Against Quasi-1D Exact Analytical Solution

While both time step and grid size introduce tradeoffs between overall accuracy and computational time (Fig. 4), ParaPower rapidly converges to closely approximate the exact analytical solution for a quasi-1D melting process ($\boldsymbol{L_2 \leq 0.1}$, $\boldsymbol{L_\infty \leq 1}$) within a relatively short computational run time (<10 s). Both the $\boldsymbol{L_2}$ and $\boldsymbol{L_\infty}$ norms were calculated from the analytical solution across increasing refinements of the grid size and time step (Eq. 3, 5). The $\boldsymbol{L_2}$ norm is calculated at the last time step for a number of successive grid sizes (Fig. 4A) and time steps (Fig. 4B). For determining the norms and order of convergence for grid spacing, the finest timesteps were used, and the finest grid spacing was used when determining the norms and order of convergence for timestep.

As the grad spacing decreases, the $\boldsymbol{L_2}$ and $\boldsymbol{L_\infty}$ norms decrease monotonically until a grid spacing of 0.04 mm, after which there is no further decrease in error with a decrease in grid spacing (Fig. 4A). At grid spacings >0.04 mm, a decrease in the overall grid spacing of nearly 2 orders of magnitude is accompanied by a less than factor of 2 increase in the overall computational time. The resulting temperature profiles at the end of the run for different grid spacings and for the exact analytical solution (the so-called 2-region melting problem calculated for a semi-infinite medium) are illustrated in Fig. 5, clearly illustrating the overall accordance of the temperature profiles calculated in ParaPower using less than 0.04 mm grid spacings.

The time discretization follows a similar trend, monotonically decreasing from time steps of ~100 to 0.1 ms, accompanied by a monotonic increase in the computational time of ~2 orders of magnitude over that range (Fig. 4B, D). As opposed to the spatial discretization, both $\boldsymbol{L_2}$ and $\boldsymbol{L_\infty}$ norms continue decreasing over the entire range of time discretization.

However, the order of convergence decreases steadily from ~0.8 at large time steps, to ~0.2 at small timesteps (Fig. 4D). Very low order of convergence at timesteps >0.1 s is attributable to numerical artifacts associated with calculating melting via a single-temperature enthalpy method approach, and suggest unreliable results at such large time steps.

Comparison Against 3D Numerical Solution

Geometry 2 was used to generate $\boldsymbol{L_2}$ and $\boldsymbol{L_\infty}$ norms and the orders of convergence as a function of both grid spacing and time step. As an analytical solution does not exist for this geometry, the $\boldsymbol{L_2}$ and $\boldsymbol{L_\infty}$ norms compare successively refined grid sizes and time steps. Figure 6A shows the error norms for grid spacing refinement, as well as the runtime for each simulation; Figure 6C displays the order of convergence for the error norms with grid size. For time step refinement, figures 6B and 6D show the error norm and simulation time, and order of convergence, respectively.

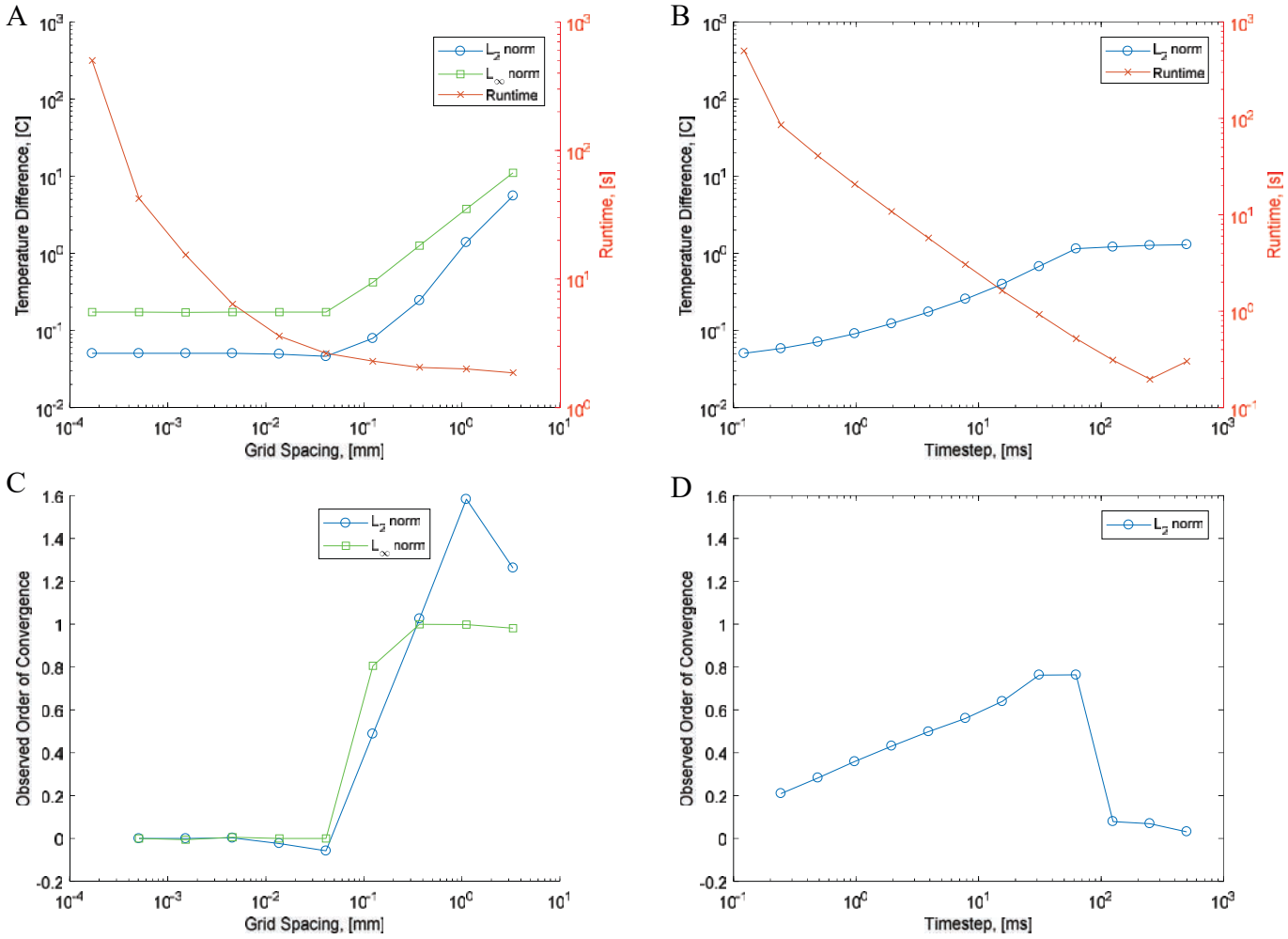

Fig. 4 Analysis of 1D numerical solution against the analytical solution: A) error metrics and runtime for different grid spacings calculated at the finest time step (dt = 0.12 ms), B) order of convergence for the metrics in A, C) L_2 norm and runtime for timestep refinement at finest grid spacing, D) order of convergence for the metrics in C

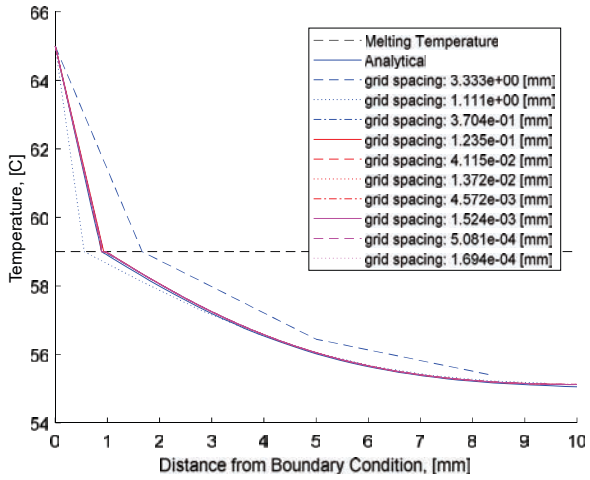

Fig. 5 Vertical temperature profiles for different grid spacings (dx = 3.33 to 1.69×10^{-4} mm).

Geometry 3 was used to compare the 3D temperature profiles and melt front positions to an equivalent simulation completed in ANSYS. The temperature (Fig. 7) and melt front profiles (Fig. 8) are shown at the final time step (t = 1 s). In both cases, ParaPower qualitatively compares well across the entire simulated domain. Furthermore, the melt front propagates a similar distance in both cases. In particular, the curvature of the melt front near the sharp corners associated with the edges of the finite heater pad is conserved across both cases. These observations support the validity of 3D melting fronts for arbitrary spatial distributions of PCM, conducting, and insulating phases.

DISCUSSION

In the case of finite difference methods, the formal order of accuracy is determined by truncation error analysis [16]. This order of convergence is determined by the methods used by the solver, and as such should be problem independent as long as the problem can be described by the physics modeled, and the restrictions of the solver are followed. For an implicit Euler solver describing transient heat transfer in the conduction

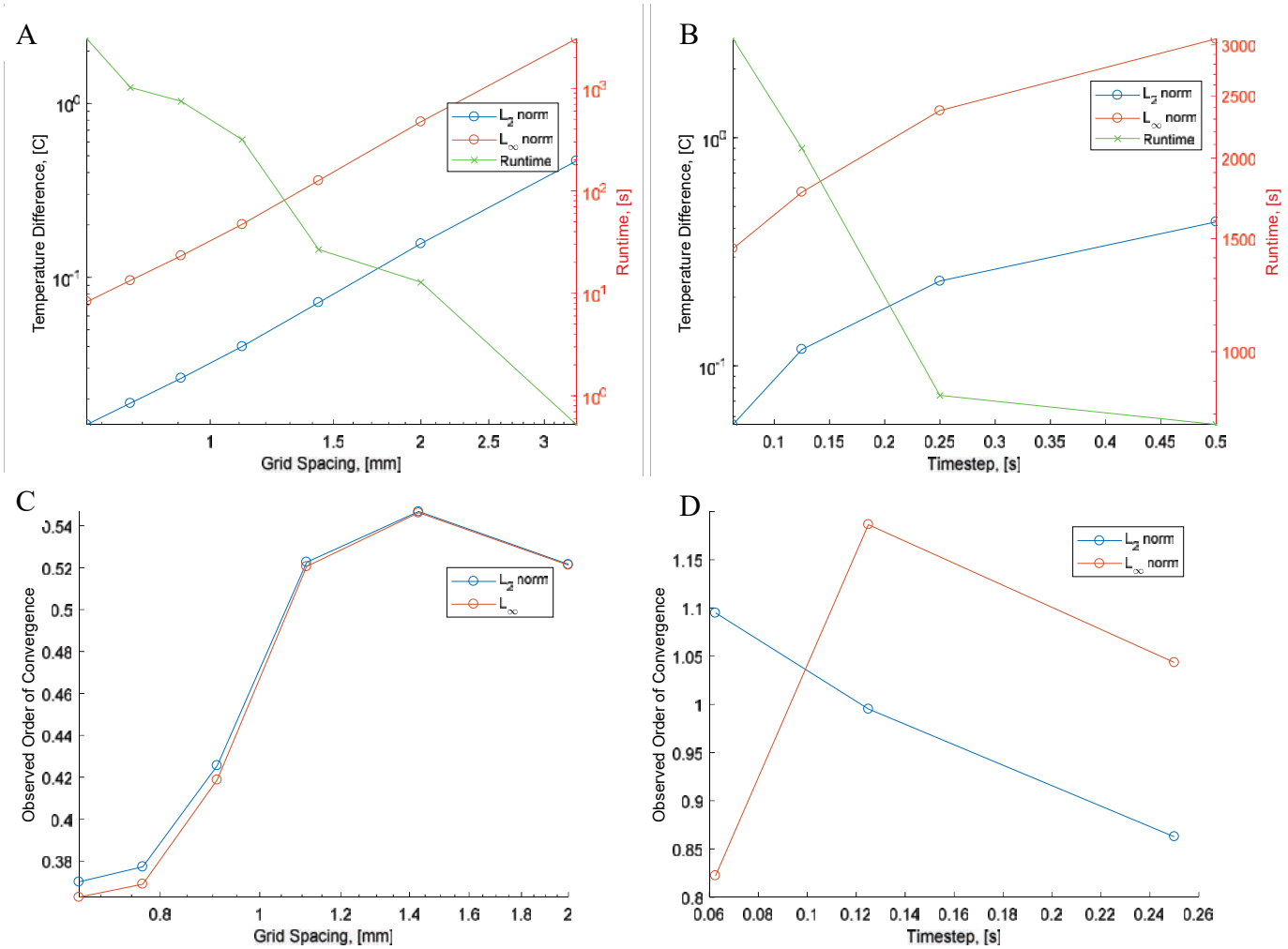

Fig. 6 Analysis of 3D numerical solution against consecutive refinements in itself: A) error metrics and runtime for grid spacing refinement at the finest timestep (dt = 30.3 ms), B) order of convergence for the metrics in A, C) error metrics and runtime for timestep refinement at finest grid spacing (dx = 0.59 mm), D) order of convergence for the metrics in C

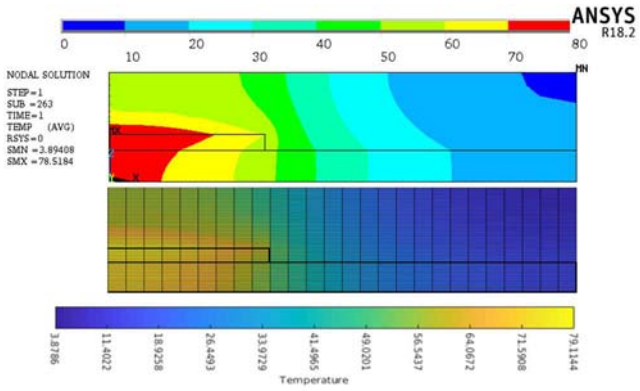

Fig. 7 Cross section comparison of the temperature profile within ANSYS(top) and ParaPower(bottom)

of a solid, these orders of convergence are expected to be constants of 2 with respect to grid spacing and 1 with respect to time step. However, this is not what has been observed by ParaPower. It is believed that the nonlinear response of the melting in PCMs is the reason for this, as the implicit Euler scheme is inherently linear, and the nonlinear response may be

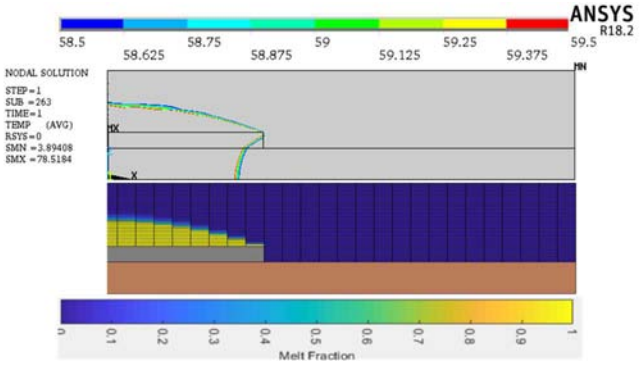

Fig. 8 Cross section comparison of the melt front between ANSYS(top) and ParaPower(bottom)

adding additional error. However, ParaPower does have a positive order of convergence for both the 1D and 3D cases, and for both refinements in grid size and time step. In addition, ParaPower demonstrates good agreement with the ANSYS model. This suggests that ParaPower can be an accurate tool for simulating phase change materials. Figures 2 and 3 suggest that for pure PCM and 1D, there is an optimal spatial discretization at which further refinement grants no benefits, as indicated by the near zero order of convergence. There is no noticeable improvement in agreement between the models as discretization is refined further once a grid size of about 0.03 mm is reached. Further grid spacing refinements only increase computation time as a rough function of N^2. Theoretically, further refinements in discretization should result in decreasing amounts of error with diminishing returns. As the error due to discretization diminishes, other sources of error can dominate. This suggests that another source of error that remains constant with spatial discretization refinement may be present in the simulations.

In the 1D simulation, ParaPower is capable of converging to an average error of less than a 0.1 °C difference to the analytical solution with a grid size on the order of 0.1 mm as shown In Figure 3a. This is further demonstrated by Figure 5, where the temperature profile of grid sizes equal to or less than 0.1 mm become indistinguishable to the analytical solution. The runtime for such a simulation is less than 10 seconds, making such computations cheap. A similar case holds true for the 3D geometries, in which an L_2 norm of less than 0.1 °C was obtained with a grid size of about 1.4 mm with a runtime of around 20 seconds. These fast simulations can allow ParaPower to test many iterations of a design to identify trends within a design space and interesting configurations for more rigorous study for a cheap computational cost.

The accuracy is a function of the discretization, disequilibrium, and geometric complexity. With all else remaining constant, as the grid spacing and timestep size decrease, the accuracy increases. This allows a user with similar simulations and prior knowledge to tailor the accuracy of the simulations. For example, if a user desires to replicate the first simulation while having an error of no more than 1 °C anywhere, the grid spacing should be approximately less than 2×10^{-4} m if using the 0.12 ms, as per figure 3a. Increasing the grid spacing or time step refinement has the cost of increased runtime, so a compromise must be balanced between accuracy and expediency.

CONCLUSION

ParaPower has demonstrated convergence to the analytical solution for a two phase melting region problem, and demonstrates positive order of convergence on a 3-dimensional multi-material problem. This suggests that the underlying physics in ParaPower are correctly implemented, but the lack of duplication of the theoretical order of convergence suggests there are many opportunities for improvements. Further work can be done quantifying these sources of error. ParaPower has demonstrated the ability to converge to an average error of less than 0.1 °C while retaining a run time of less than 10 seconds. This indicates that ParaPower possesses the potential to perform many simulations in a short period of time, making it suitable for first-pass parametric analysis. The relationship between discretization and the L_2 and L_∞ norms is explored, allowing users to make a more informed decision when deciding on discretization. Together, this indicates a promising beginning to a parametric design tool for simultaneously computing thermal, mechanical, and electrical phenomenon in electronics packaging. ParaPower remains in heavy development at the Army Research Laboratory.

Acknowledgements

The authors would like to thank the Office of Naval Research, the U.S. Army Research Lab, the Office of the Secretary of Defense, and Bruce Geil for their support in this work. Deckard acknowledges support of this work from the Office of Naval Research (ONR) grant N00014-17-1-2802.

References

[1] S. Garimella et al, “Thermal Challenges in Next-Generation Electronic Systems”, IEEE Transactions on

Components and Packaging Technologies, vol 31, pp 801-815, 2008.
[2] E. Laloya et al, “Heat management in Power Converters: From State of the Art to Future Ultrahigh Efficiency Systems”, IEEE Transactions on Power Electronics, vol 31, pp 7896-7908, 2016.
[3] T.J.Zhang et al, “Two-phase refrigerant flow instability analysis and active control in transient electronics cooling systems”, International Journal of Multiphase Flow, vol. 37, pp 84-97, 2011.
[4] Z. Yang et al, “Model Predictive Control of Vapor Compression Cycle for Large Transient Heat Flux Cooling”, American Control Conference, 2016.
[5] D. Gonzalez-Nino et al, “Experimental Evaluation of Metallic Phase Change Materials for Thermal Transient Mitigation”, International Journal of Heat and Mass Transfer, vol. 116, pp 512-519, 2018.
[6] D. Gonzalez-Nino et al, “Numerical Evaluation of Multiple Phase Change materials for Pulsed Electronics Applications”, ASME. Heat Transfer Summer Conference, 2016.
[7] L. Boteler and S.M. Miner, “Power packaging thermal and stress model for quick parametric analyses,” Proceedings of the ASME 2017 International Technical Conference and Exhibition on Packaging and Integration of Electronic and Photonic Microsystems Conference (pp. V001T04A012-V001T04A012), 2017.
[8] L. Boteler and S.M. Miner, “Comparison of Thermal and Stress Analysis Results for a High Voltage Module Using FEA and a Quick Parametric Analysis Tool,” Proceedings of the ASME 2018 International Technical Conference and Exhibition on Packaging and Integration of Electronic and Photonic Microsystems Conference (pp. V001T04A019-V001T04A019), 2018.
[9] L. Boteler and A. Smith, “3D Thermal Resistance Network Method for the Design of Highly Integrated Packages”, Proceedings of the ASME 2013 Heat Transfer Summer Conference, 2013.
[10] V.R. Voller et al, “An Enthalpy Method for Convection/Diffusion Phase Change”, International Journal for Numerical Methods in Engineering, vol. 24, pp 271-284, 1987.
[11] C.R. Swaminathan, and V.R. Voller, “On the enthalpy method,” International Journal of Numerical Methods for Heat & Fluid Flow, 3(3), 233-244, 1993.
[12] J.M. Hill, *One-dimensional Stefan problems: an introduction*, *in* Pitman Monographs and Surveys in Pure and Applied Mathematics, v. 31. New York, NY, 1987.
[13] H. Hu and S.A. Argyropoulos, “Mathematical modelling of solidification and melting: a review,” Modelling and Simulation in Materials Science and Engneering, vol. 4, pp. 371-396, 1996.
[14] A. Lipchitz et al, “Determination of Specific Heat of Eutectic Indium-Bismuth-Tin Liquid Metal Alloys as a Test Material for Liquid Metal – Cooled Applications,” Applied Mechanics and Materials, vol. 420, pp 185-193, 2013.
[15] A. Lipchitz et al, “Experimental Investigation of the Thermal Conductivity and Viscosity of Liquid In-Bi_Sn Eutectic Alloy (Field’s metal) for use in a Natural Circulation Experimental Loop”, 23rd International Conference on Nuclear Engineering, 2015.
[16] C.J. Roy, “Review of code and solution verification procedures for computational simulation,” Journal of Computational Physics, vol. 205, pp 131-156, 2005.